CONF-830845--7

BNL-NUREG-33657

BNL-NUREG--33657

DE84 000623

Initiation and Propagation of Stress-Corrosion Cracking of Alloy 600 in High-Temperature Water

R. Bandy and D. van Rooyen

Materials Research Group
Brookhaven National Laboratory
Upton, NY 11973

ABSTRACT

Results of stress-corrosion cracking data are presented for Inconel 600 steam-generator tubing. U-bend, constant-load, and slow extension-rate tests are included. Arrhenius plots are presented for failure times vs. inverse temperature for crack initiation and propagation. Effect of applied load is expressed in terms of log-log curves for failure times vs. stress, and variations in environment and cold work are included. Microstructure and composition of oxide films on Inconel 600 surfaces were examined after exposure to pure water at 365°C, and stripping with the bromine-methanol method. Results are discussed in terms of transient creep, film rupture and a mass-transport-limited anodic process.

INTRODUCTION

Alloy 600 tubes have generally performed well in PWR steam generators under normal operating conditions. However, occasional leaks resulted from stress corrosion cracking (SCC), related to the presence of unusually high residual or operating stresses, or to abnormal secondary side chemistry. The suspected high stresses can result from either the deformation of tubes during manufacture, or distortion during operation e.g. from denting. The present research examines the factors involved in the SCC of Alloy 600 in high temperature, deaerated water, with the objective of developing empirical data that will relate life expectancy of tubing i.e. SCC times, to factors such as stress, strain, strain rate, environmental conditions, microstructure and cold work of the metal. Corrosion tests address two simulated conditions, i.e., 1) where deformation occurs but is no longer active, such as when denting is stopped, and 2) where slow plastic deformation of the metal continues, as would occur during denting. Laboratory test media consist of pure water as well as solutions to simulate environments that would apply in service; they are deaerated before start-up to give O_2 analyses in the range 0-5 ppb. Tubing from actual production is used in carrying out these tests. Examination of structure includes metallography and extraction replicas.

EXPERIMENTAL

The details of autoclave testing, specimen preparation, materials and their composition have been described in earlier publications of results under this program(Ref. 1-3).

RESULTS AND DISCUSSION

U-Bend Tests

An interesting correspondence is found between crack velocity calculated from crack lengths observed in U-bends and in CERT tests. Although the U-bend calculations are not very precise, there is little question they are in the same region as the crack velocities in CERT at the same temperature: U-Bends at 365°C $\fallingdotseq 6 \times 10^{-7}$ mm.sec^{-1};CERT $\fallingdotseq 8 \times 10^{-7}$ mm sec^{-1} at 365°C. (See also the section on CERT data for more details on variations in crack propagation rate).

Earlier results of U-bend tests done in pure H_2O suggested that the carbon level of Alloy 600 could possibly influence crack initiation /temperature relationships. Specifically, activation energy seemed to increase with increasing carbon content, based on cracks observed with tubes of 0.01-0.05% carbon in the temperature range 325 to 365°C, with most of the data from the higher temperature end. More data are due at lower temperatures of 290 and 315°C.

For the purpose of this paper, an update is made of the present state of the U-bend tests at BNL, as given in Fig. 1. No SCC has yet been seen at 290°C and 315°C in test times exceeding 100 weeks. For the 0.02% carbon material, one test group at 290°C and another at 315°C have just exceeded, without SCC, the times at which SCC would have been predicted by extrapolation from high temperature curves*. Thus, at least for this material, the activation energy at lower temperature may exceed the 36 Kcal/mole value that was reported(3). A few older exposures have reached almost twice this time at 290°C, but only duplicates were originally placed in this test, so that it will not be statistically as valuable as the other group now at 100 weeks.

A general trend may be expected, therefore, in support of the findings of G. Theus(4)that the Arrhenius curves do, in fact, become steeper in the region of operating PWR steam generator temperatures. It should be kept in mind that U-bend tests do not allow an accurate estimate of stress relief during exposure, which may contribute to the longer SCC times that are observed in the long-term autoclave tests. An interesting observation in this regard, also, is that tubing under high constant load cracks quicker than corresponding U-bends, probably because stress in not relieved.

CERT Tests

CERT data show that this method does not fully eliminate the initiation stage of SCC, i.e., cracks do not start when the test begins, nor, in fact at the onset of plastic deformation; it takes a finite time (after yielding) for SCC to develop.(1,2) Initiation times are, however, much shorter than for U-bends, and vary with temperature. Figs. 2, 3 show a family of straight line Arrhenius plots of CERT data, obtained at strain rates of about 2 to 3 x 10^{-7}sec^{-1}. A heat of 0.01%C was used for most of these data, although another heat of low carbon and one of 0.05%C agree in general with the slopes given here, and an activation energy of about 33 Kcal/mole can be calculated for material as cold worked, or aged (365°C), or mill annealed, suggesting that these treatments do not affect the crack propagation mechanism. Variations in crack propagation rates appear to be due to a change in the constant in the Arrhenius equation.

We have used a method of extrapolating plots of crack length vs. strain (down to zero crack length) in order to determine the point at which SCC starts. While this seems to give a reasonable basis for estimating crack velocities, it is not believed to be accurate enough for reliable estimates of strain required to induce SCC initiation. We are adopting more direct measurements for this purpose.

Temperature exerts a much greater influence than strain rate on crack velocity. Most of the present tests are conducted successfully at about 2-3x10^{-7}sec^{-1}, but for test conditions where cracks grow slowly, a lower strain rate can give better crack length measurements by allowing more time for cracks to penetrate. For instance, very deep cracks were found at 9 x 10^{-8}sec^{-1} in one case, compared to insignificant crack depths at 3.5 x 10^{-7}sec^{-1}.

Cold work increases SCC velocity (Fig. 2). At 20% cold work, the results fall close to the data points earlier found for flattened pieces in pure H_2O. The points for 5% cold work in pure H_2O + H_2 and simulated primary water fall within 2 to 3.5 x 10^{-6} mm sec $^{-1}$ at 365°C and appear to follow the same slope, Q = 33 Kcal/mole, as earlier found and shown in Figs. 2 and 3. For cold worked material, the effect of environment seems to be masked by the

---

*In the present plots, no distinction has been made between pickled and unpickled specimens of the 0.02%C heat. These two groups will be plotted separately later when final data become available.

increase in crack velocity due to the prior cold reduction. Data from more electrolytes than were covered previously have been added to this paper(3).

In the case of U-bends, it was indicated that hydrogen added to the test medium increased the stress corrosion crack initiation frequency. As shown in Fig. 3 the same tendency appears to be present in the CERT results, at least

in the case of the as-received material where we observed the greatest spread between the various curves obtained from different environments. Opposed to this hydrogen effect appears to be a lowering in the crack velocities due to an increase in pH such as would result from the addition of lithium hydroxide to the test medium. As a result it appears that simulated primary water is not substantially different from pure water in this particular test procedure. In all cases the curves appear to be of about parallel slope, again giving rise to the same activation energy that was mentioned above. In the case of boric acid and lithium hydroxide, we observed somewhat more scatter than usual in our test data. The reason for this is not clear. Cold work has an effect of increasing crack velocity in Inconel 600 in the CERT test as shown in Fig. 2 and also as mentioned in the previous paragraph. Consequently, variations in the environment are not quite as readily analyzed for the cold worked material.

Constant Load Tests

For the case where denting or active deformation is no longer occurring, it is necessary to obtain data that relate failure times to stress, i.e., the load on the tube. In service, these stresses can consist of residual plus operational stress, and may be complex. Tests in progress use simulated dents in Inconel 600 production tubing, but so far they have been exposed for too short a time to give SCC. In the present constant load test series, another attempt at relating stress level to SCC failure time is made by means of tensile specimens under constant applied load. This will of course be compared to the simulated dents in order to find out if quantitative stress values can be assigned to failure in Alloy 600. Figures 4 and 5 show a band within which failure times could be plotted on a logarithmic scale against stress, in pure H_2O for as-received material. As earlier reported, the slope of the log-log curve gives -4 as the power of stress to which failure time is proportional. Data obtained from other environments with as-received Inconel 600 production tubing at 365°C fall generally in or very close to the pure water band in Fig. 5. One interesting observation is that the adverse H_2 effect on SCC, as seen in U-bends, has not been evident in constant load experiments.

Lowering the test temperature to 345°C increases the failure times, and these points fall outside the 365°C scatter band. Both tests used as-received tubing with 0.01%C. Assuming a semi-log inverse temperature relationship, with failure time, ($T_F = k.\exp^{-Q}$) the two data points led to a calculated activation energy for SCC under constant load of 34 Kcal/mole. Although only two points are available, this value is remarkably close to the CERT and U-bend values for 0.01%C Inconel 600. At low carbon levels, therefore, the mechanisms of crack initiation and propagation could be very closely related.

In constant load tests, some of the 20% cold worked specimens failed in about the same time as the as-received tubing in pure H_2O at 365°C, and some of the 5% cold worked specimens cracked in one or two days, i.e. much more quickly. Unfortunately, no trend could be established because of scatter in the data. In producing the test specimens, the cold work was introduced by mechanical wall thinning while holding the tube over an internal mandrel. The yield points of the individual specimens subsequently cut from the cold worked tube are raised, during this process, but there is a considerable variation from one individual specimen to another. It is not surprising, therefore, that data plots of load, (as a fraction of the as-received, room temperature yield point) vs. failure times do not reveal any reliable overall trend. An increase in SCC susceptibility due to cold work is apparently offset by the fact that the actual applied load is a much lower fraction of the true yield point than of the as-received value of the yield point. This scatter cannot be explained further without measuring the properties of each test piece at the test temperature. As suggested below, it is also possible that the maximum effect of cold reduction may result from intermediate levels of cold work.

Comparison of Methods

There is evidence that all heats of susceptible Inconel 600 do not necessarily respond by cracking in SCC tests using simple tensile specimens. Some heats have cracked easily only as U-bends and with difficulty or not at all in one (or both) the constant load test and CERT. In the case of CERT, it may be that the strain rate range we used was not suitable, but it is more likely that a more complex stress is needed. We have designed experimental procedures to follow the latter possibility quantitatively.

Oxide Film and its Role in SCC

Extraction replicas of oxides and precipitates were studied after film removal in a start to understand the role of microstructure: part of this ongoing work is described here.

A piece of Alloy 600 specimen cut directly from a tube was immersed in deaerated, pure water at 365°C for about two weeks. After withdrawal, the specimen was shadowed with carbon (to avoid shattering) and the surface film was stripped using a 10% bromine-methanol solution. The film was mounted on a copper grid and analyzed on a JEOL 100 electron microscope. Fig. 6 shows a typical micrograph of the film consisting of several components some of which appear to have regular crystallographic patterns giving well defined diffraction patterns as shown in Fig. 7. Note in Fig. 6 that the growth of the film appears to be different in different grains, perhaps influenced by orientation. It is clear that the film retains the grain boundaries of the substrate and therefore fracture might be expected to follow the boundary, a plane of weakness especially in mechanically weak substances.

Grain boundaries could influence SCC in a number of ways. First, strain is likely to be greater near the grain boundary which may also be the site of numerous dislocation pile-ups. Second, the composition of the grain boundary may differ from the bulk composition. Thus, in a narrow region at or adjacent to the grain boundary, an anodic area may be postulated, especially if there is large misorientation between abutting grains or segregation of a particular species at the boundary.

Fig. 8 shows a typical EDX analysis of the film shown in Fig. 6. A strong nickel peak suggests that nickel enrichment has occurred due perhaps to preferential dissolution of nickel. The strong copper signal came from the grid holding the sample. A compositional analysis of the surface film by X-ray photoelectron spectroscopy is currently underway and will be presented at a later date.

The specimen, under an optical microscope (before stripping), exhibited strong interference colors suggesting that the film was relatively thick and presumably much thicker than 0.7 x 10^{-5}cm reported by Vermilyea (5) for Alloy 600 in oxygen free pure water at 289°C where SCC did not occur.

The film is perhaps porous and not perfectly protective. Cowan and Staehle (6) studied the polarization behavior of pure nickel as a function of pH and temperature up to 300°C. In a pH 6.3 solution (0.1N K_2SO_4), current in the primary passive region was found to increase with potential, indicating a non-protective film. Above a certain threshold temperature (130°C in this case), they observed an abrupt loss of active to passive transition and the anodic curve had the shape expected for a diffusion controlled process, arising from the dissolution of nickel through the pores of the nickel oxide film.

Thermodynamic considerations and experimental observations indicate(6) that in high temperature deaerated water, Inconel 600 has a corrosion potential equal to that of the hydrogen redox potential, and at partial pressure of hydrogen equal to one atmosphere, there is no driving force for the corrosion of pure nickel at neutral pH. However, thermodynamic data also suggest(6) that the electrochemical potential of the reaction:

$$Ni + H_2O = NiO + 2H^+ + 2e$$

approaches the hydrogen redox potential as the temperature increases from 25 to 300°C. Thus NiO can be formed directly if the temperature is raised even further or potential of the specimen raised by adding oxidizers or by external polarization, or the hydrogen partial pressure is reduced. On the other hand, if a hydrogen overpressure is maintained, NiO formation would be impeded. This may be one of the factors behind the results that Alloy 600 generally does not crack in high purity water overpressured with hydrogen(7). (This contrasts with our observations, although at a somewhat lower H_2 level, that cracking is actually accelerated by H_2.)

For SCC to occur on a film-covered specimen, a mechano-chemical model(5,8) may be envisaged. In a stressed sample, the creep in the metal ahead of the film may be considered to introduce increasing elastic strain in a mechanically weak film, eventually leading to fracture. The crack is arrested by plastic deformation when it enters the substrate and the environment again will have direct access to the metal, leading to fresh oxide film formation. The process is repeated leading to discontinuous crack propagation. In the model described above, it is assumed that the creep rate at the crack tip would be greatly influenced by the magnitude of the local stress. Also, the activation energies for region I and II (in a crack velocity (V) vs. stress intensity (K) curve) of crack growth would generally correspond to those for transient creep and a mass-transport-limited anodic dissolution process, respectively.

Speidel(9) and Blackburn et al.(10) have discussed the activation energy question for SCC in various alloy-environments. For many aluminum, magnesium and titanium alloys in aqueous halide media, organic solvents, and molten salts, activation energies near 4 KCal/mole have been measured in stage II crack growth(9). For region I, however, the activation energies are about 27 to 28 KCal/mole for titanium, aluminum alloys and glass(9,10). Ohtani and Hayashi(11) reports an activation energy of 20-23 KCal/mole for stainless steel - $MgCl_2$ system. For aluminum alloys, Speidel(9) gives the SCC velocity in stage II region as:

$$V = C_2 \exp[(-Q/RT)]$$

where Q is the apparent activation energy C_2 is another constant, R and T have usual meanings.

For stage I, however, the above equation is modified to

$$V = C_3 \exp\ (-Q + C_4 K_I)/RT$$

where C_3, C_4 are constants, Q is the activation energy and K_I is the crack tip stress intensity.

Thus, a time-to-failure test would generally give an apparent activation energy between 4 and 28 KCal/mole, but biased towards the higher value because most of the life time of the specimen is probably spent in the slow growing region I. The high activation energy (~33 KCal/mole) observed in our system implies that the SCC in high purity water is influenced primarily by a mechanical processes involving transient creep(5). Thus thermal treatments of the alloy which will influence the dislocation motion and modify the creep behavior are likely to influence the SCC behavior.

Influence of Cold Work

According to the model described above, cold work should affect the SCC behavior because of its influence on creep rate and because some grains would be left in residual tension as a result of cold work. The degree of cold work is also a very important parameter. Thus, small amounts of cold work is likelikely to increase dislocation density and creep rate and will thus increase the propensity to SCC. Large amounts of cold work on the other hand may produce dislocation structures in which few free dislocations are available and in which transient creep may be small. This is consistent with the results of our constant load tests where specimens with a small amount of cold work (~ 5%) underwent the most rapid failure, whereas specimens with 20% cold work (~ 20%) took a much longer time.

Our results are in conformity with those of Foster and Taylor(12). In their tests in degassed pure water at 300 and 350°C, they noticed that C-ring samples with less than 5% cold work were more susceptible to SCC than U-bend samples made from longitudinal strips cut from the tubing, resulting in 15 to 20% cold work. Except for the cold work level, all other aspects of the tests were identical.

SUMMARY

Work is described involving an ongoing stress corrosion program aimed at developing quantitative relationships between factors involved in stress corrosion cracking (SCC) of Inconel 600 steam generator tubing.

At high temperatures, carbon seems to influence the activation energy of SCC, but this effect is not yet confirmed at lower temepratures (290-315°C). Tests underway without SCC (in U-bends) so far have reached the stage where they may fit better with a changing activation energy (Q), higher at 290-300°C, than with a constant value over the range studied (290-365°C).

Constant extension rate tests (CERT) continue to show an activation energy around 30 Kcal/mole for crack growth rate. Environment and cold work affect crack growth rate, but do not seem to have a significant effect on Q. Cold work is adverse, and also tends to mask the effects of changing environments.

Constant load information shows failure time to be proportional to the inverse fourth power of stress. Cold work is adverse in these tests also.

Oxide films were analyzed for structure and composition after stripping from Inconel 600 subsequent to high temperature, deaerated water exposure. Nickel enrichment was found, and these films may be somewhat thicker than reported in the literature(5). Well defined diffraction patterns are being analyzed. The oxide retains the substrate grain boundaries, and these may be weak areas if slow creep occurs. Cracking is discussed in terms of transient creep and mass-transport-limited anodic dissolution.

ACKNOWLEDGEMENTS

Work supported by the U.S. Nuclear Regulatory Commission, Office of Nuclear Regulatory Research.

REFERENCES

1. T. S. Bulischeck and D. van Rooyen, "Stress Corrosion Cracking of Alloy 600 Using the Constant Strain Rate Test," Corrosion, Vol. 37, No. 10, pp. 597-607, NACE, 1981.

2. T. S. Bulischeck and D. van Rooyen, "Effect of Environmental Variables on the Stress Corrosion Cracking of Inconel 600 Steam Generator Tubing," Nuclear Technology, Vol. 55, pp. 383-393, ANS, 1981.

REFERENCES (cont'd)

3. R. Bandy and D. van Rooyen, "Stress Corrosion Cracking of Inconel Alloy 600 in High Temperature Water - an Update," Paper 139, NACE Corrosion 1983, Anaheim, California, April 1983 (Submitted for publication in NACE CORROSION).

4. G. J. Theus, "Summary of the Babcock and Wilcox Company's Stress Corrosion Cracking Tests of Alloy 600," EPRI WS-80-0136, *EPRI Workshop on Cracking of Alloy 600 U-bend Tubes in Steam Generators,* Denver, 1980.

5. D. A. Vermilyea, "A Film Rupture Model for Stress Corrosion Cracking," in Stress Corrosion Cracking and Hydrogen Embrittlement of Iron Base Alloys, p. 208, Firminy France, June 12-16 (1973).

6. R. L. Cowan and R. W. Staehle, J. Electrochem. Soc. *118* , 557 (1971).

7. R. L. Cowan and C. S. Tedmon in "Advances in Corrosion Science and Technology," Vol. 3, ed. M. G. Fontana and R. W. Staehle, Plenum Press, New York, p. 293 (1973).

8. E. N. Pugh, "A Film Rupture Model for Stress Corrosion Cracking," in Stress Corrosion Cracking and Hydrogen Embrittlement of Iron Base Alloys, p. 37, Firminy France, June 12-16 (1973).

9. M. O. Speidel, in "The Theory of Stress Corrosion Cracking in Alloys," ed. J. C. Scully, NATO, p. 289 (1971).

10. M. J. Blackburn, J. A. Feeny and T. R. Beck, same as Ref. 7, p. 148.

11. N. Ohtani and Y. Hayashi in "Passivity and its Breakdown on Iron and Iron Base Alloys" USA-Japan Seminar, ed. R. W. Staehle and H. Okada, p. 169 (1976).

12. C. G. Foster and J. W. Taylor, Paper No. 8, The Institute of Civil Engineers, London (1971).

Figure 1	SCC in Pure Water. U-Bends of Commercial Tubing.
Figure 2	Effect of Cold Work in CERT. Alloy 600 0.01%C
Figure 3	Environmental Effects in CERT. A.R. Alloy 600 0.01%C
Figure 4	As-received Alloy 600 Tubing. 365°C. Pure H_2O. Slope of $(T_F = k\ \mathrm{stress}^b) = -4$
Figure 5	As-received Alloy 600 Tubing. 365°C. Pure H_2O. Slope of $(T_F = k\ \mathrm{stress}^b) = -4$
Figure 6	TEM micrograph of oxide film grown on Alloy 600 in deaerated pure water at 365°C for approximately two weeks.
Figure 7	Typical diffraction pattern of the oxide shown in Fig. 6.
Figure 8	Typical EDX analysis of the oxide film showing nickel enrichment.

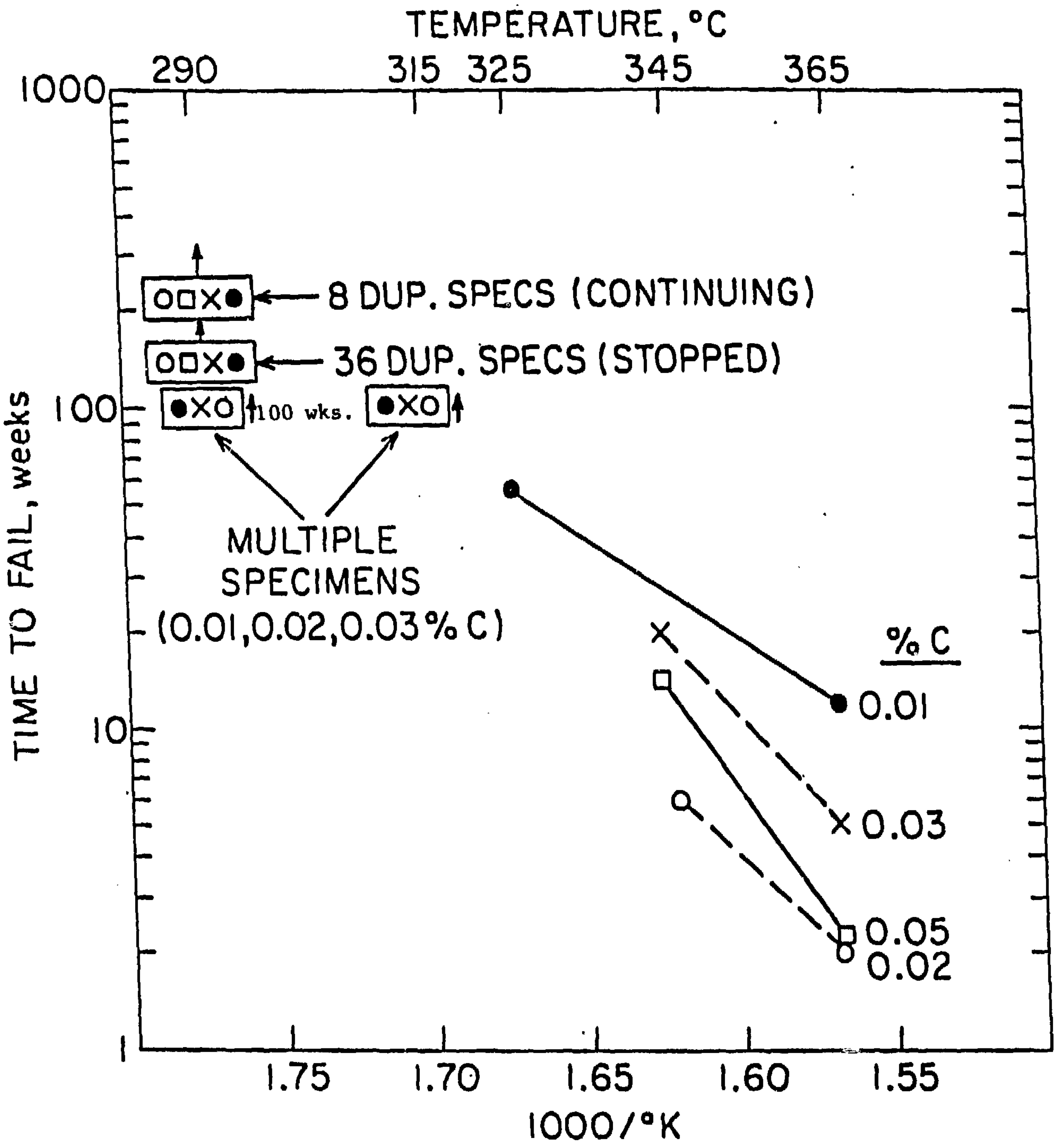

FIG. 1 SCC IN PURE WATER. U-BENDS OF COMMERCIAL TUBING

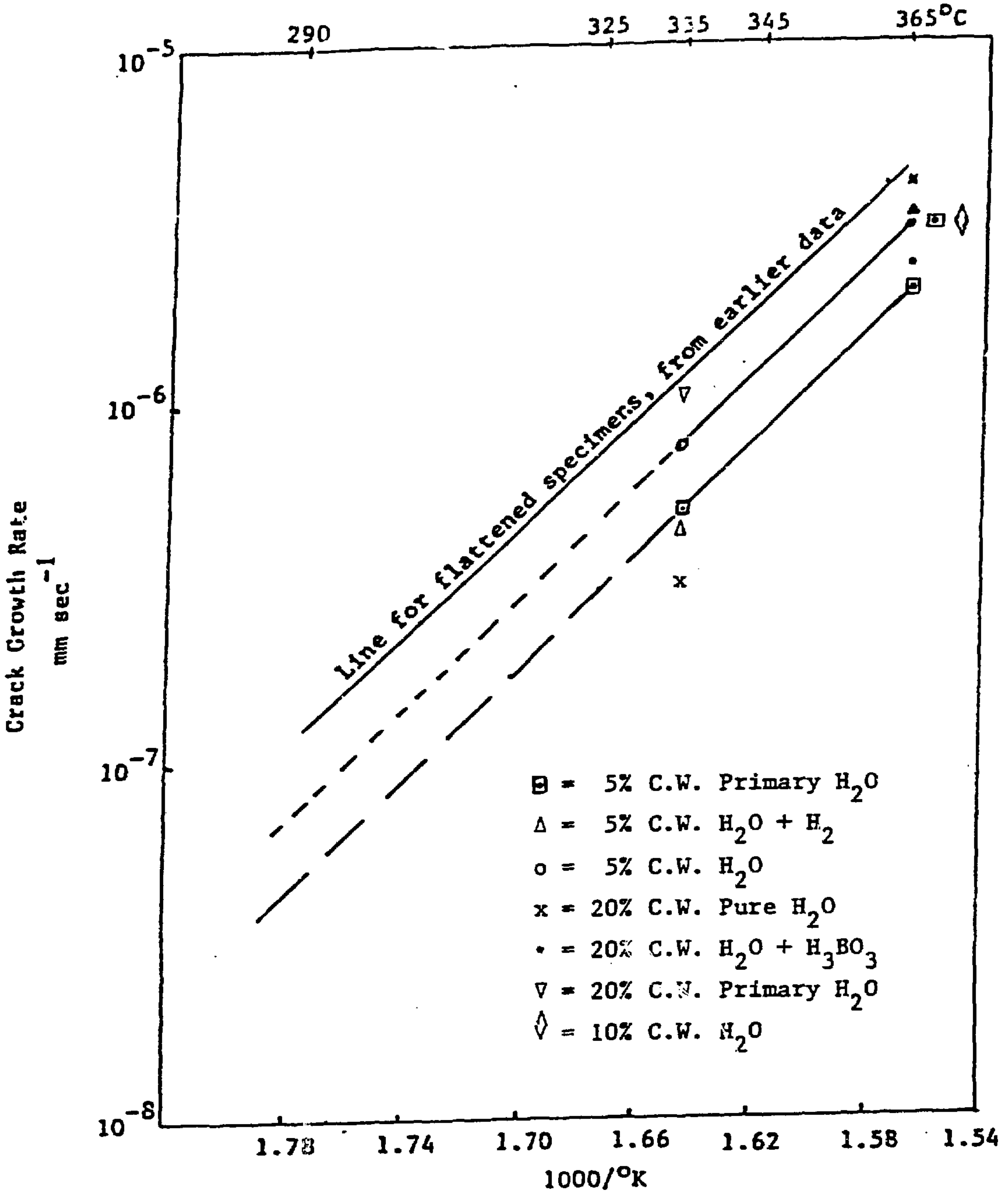

FIGURE 2. Effect of Cold Work in CERT. Alloy 600
0.01% C

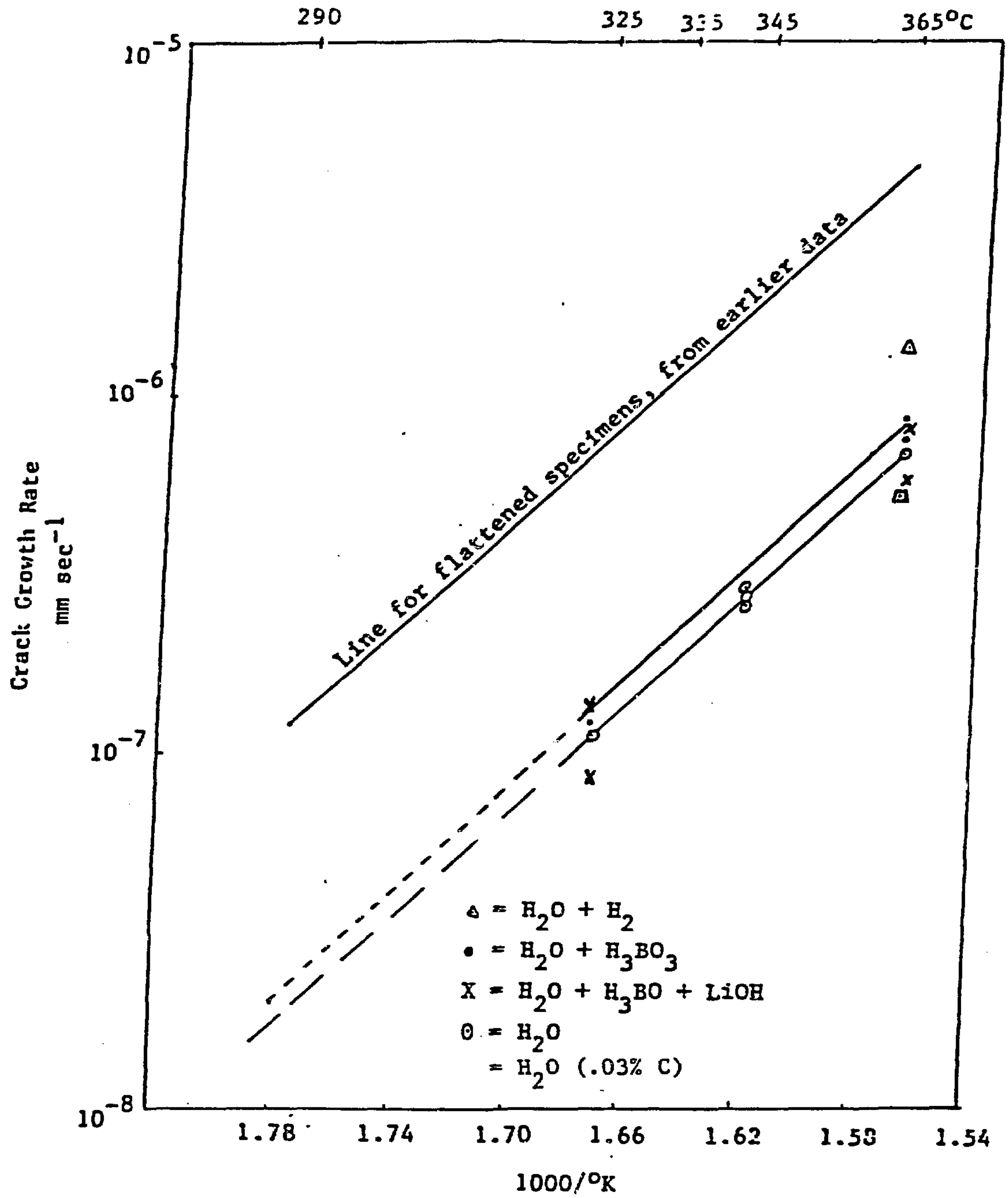

FIGURE 3. Environmental Effects in CERT. A.R. Alloy 600. .01% C

Effect of Applied Stress
on Failure Time, Pure H_2O

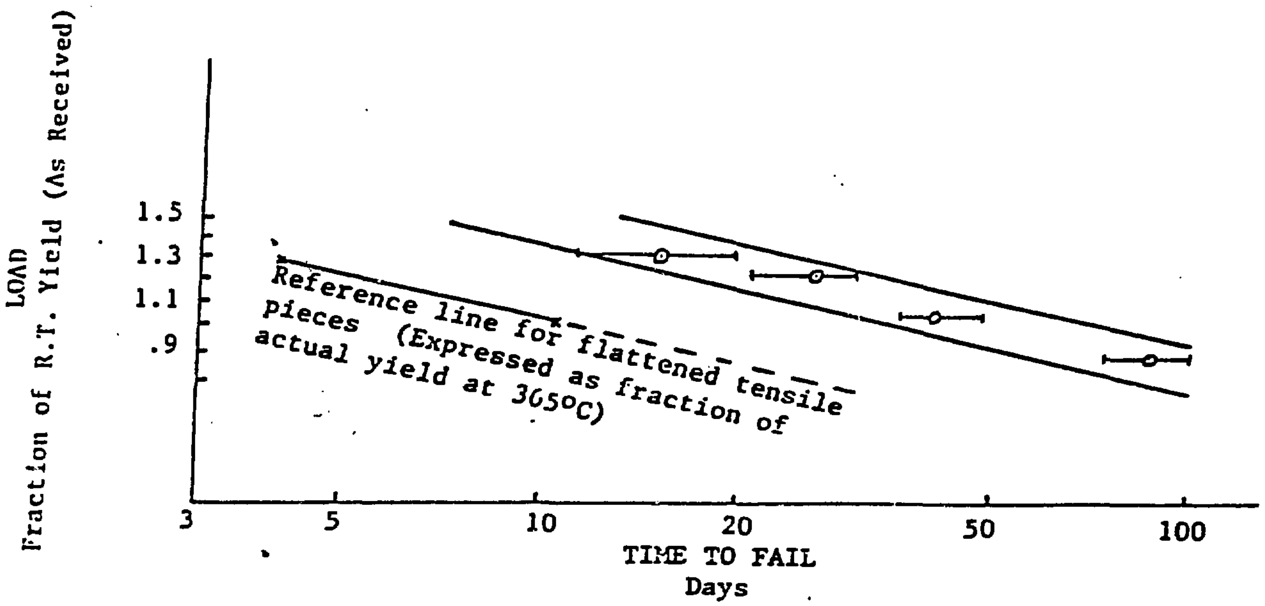

Figure 4. As-received Alloy 600 Tubing. 365°C. Pure H_2O.
Slope of (T_F = k·stress^b) = -4

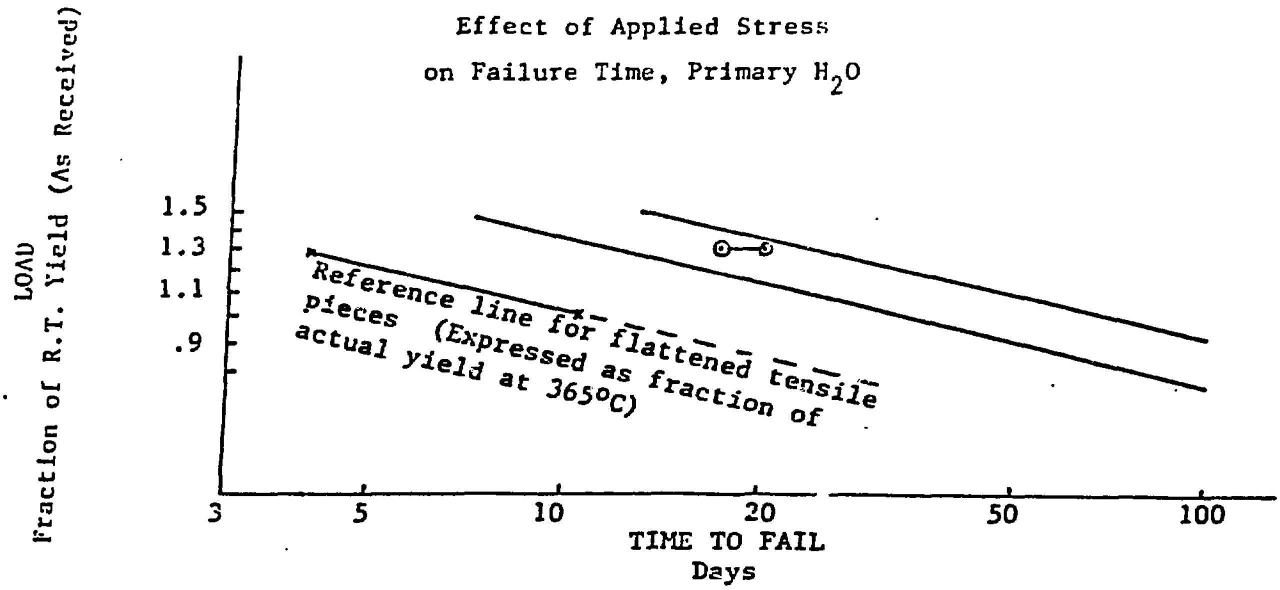

Figure 5. As-received Alloy 600 Tubing. 365°C. Primary H_2O. Failure Locations Within Band of Fig. 4

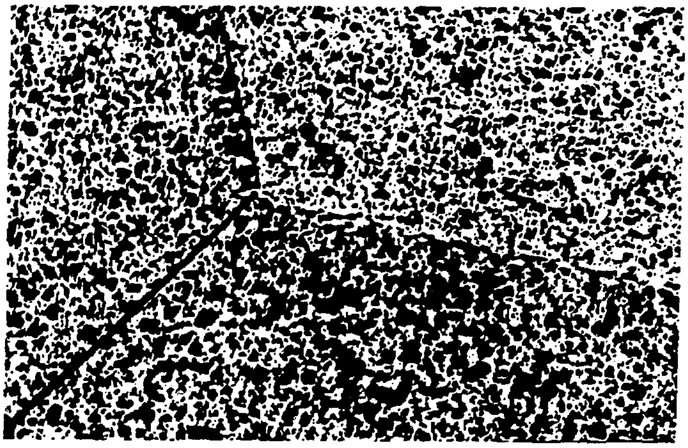

Figure 6. TEM micrograph of oxide film grown on Alloy 600 in deaerated pure water at 365°C for approximately two weeks.

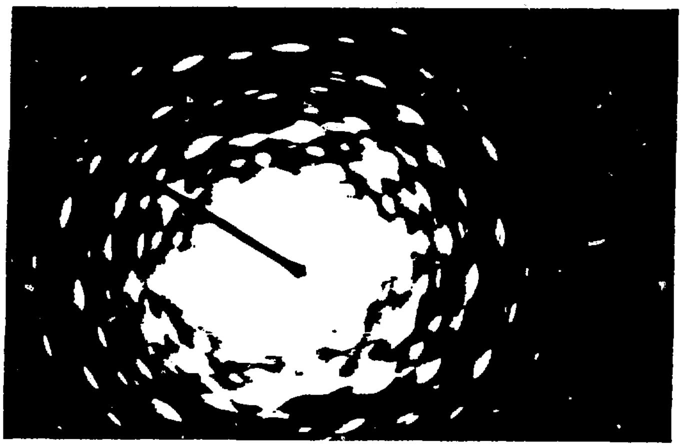

Figure 7. Typical diffraction pattern of the oxide shown in Fig. 6.

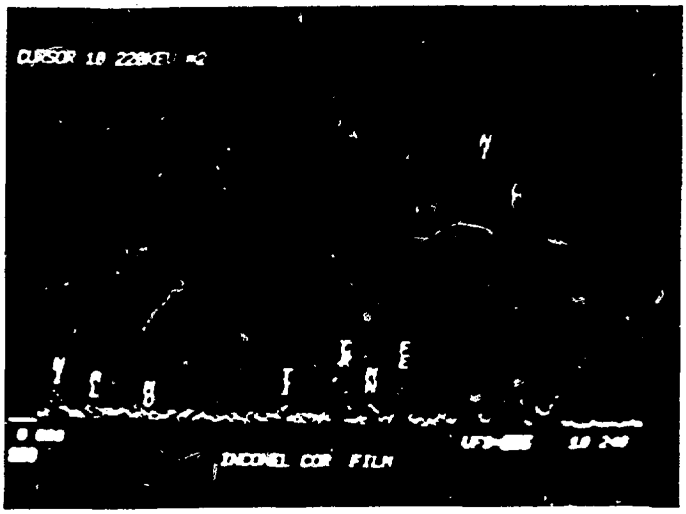

Figure 8. Typical EDX analysis of the oxide film showing nickel enrichment.